Nonadiabatic phonons within the doped graphene layers of XC_6 compounds

Mark P. M. Dean,[1,*] Christopher A. Howard,[2] Siddharth S. Saxena,[1] and Mark Ellerby[2]
[1]*Cavendish Laboratory, University of Cambridge, JJ Thomson Avenue, Cambridge CB3 0HE, United Kingdom*
[2]*London Centre for Nanotechnology and Department of Physics and Astronomy, University College London, London WC1E 6BT, United Kingdom*
(Received 23 October 2009; published 8 January 2010)

We report Raman-scattering measurements of BaC_6, SrC_6, YbC_6, and CaC_6, which permit a systematic study of the phonons and the electron-phonon interaction within the doped graphene layers of these compounds. The out-of-plane carbon phonon softens as the spacing of the graphene layers is reduced in the series BaC_6, SrC_6, YbC_6, and CaC_6. This is due to increasing charge in the π^* electronic band. Electron-phonon interaction effects between the in-plane carbon modes at $\approx$1500 cm^{-1} and the π^* electrons cause a strong nonadiabatic renormalization. As charge is transferred into the π^* band, these nonadiabatic effects are found to increase concurrent with a reduction in the phonon lifetime.

DOI: 10.1103/PhysRevB.81.045405 PACS number(s): 78.66.Tr, 63.20.−e, 71.20.Tx, 78.30.Na

I. INTRODUCTION

There is mounting evidence that the nature of electron-phonon interaction in graphitic systems is not fully understood [e.g., in graphene[1–3] or carbon nanotubes (CNTs) (Ref. 4)]. In graphite electron-phonon scattering is the main contribution to the phonon lifetime and therefore the Raman linewidth, which is typically 11.5 cm^{-1}.[5] When atoms are inserted into graphite, electrons often act to dope the graphene sheets and the Raman linewidth increases dramatically to $\sim$100 cm^{-1}. The question of the electron-phonon interaction is also interesting in light of the discovery of superconductivity at 11.5 K in CaC_6.[6,7] Measurements of a finite Ca isotope effect[8] and of an *s*-wave symmetry superconducting gap[9,10] suggests that the superconductivity is electron-phonon mediated. However, several experimental and theoretical techniques implicate different groups of phonons and electrons are responsible for the superconductivity.[8,11–16]

The adiabatic Born-Oppenheimer approximation, in which electrons are assumed to instantaneously respond to the motion of the ions, has been widely applied within the framework of density-functional theory (DFT) to predict the phonon frequencies in metals.[17] Despite this approximation not being theoretically justified, the discrepancies introduced are usually small $\lesssim$1%.[18] However, a much larger effect can be observed provided $|\boldsymbol{q}.\boldsymbol{v}_F| \ll \omega$,[18,19] where $\boldsymbol{q}$ is the phonon wave vector, $\boldsymbol{v}_F$ is the Fermi velocity, and ω is the phonon frequency. Graphene and materials composed of graphene layers typically have small $\boldsymbol{v}_F$ perpendicular to the graphene sheets. This makes these systems ideal to observe nonadiabatic effects. Weak nonadiabatic effects have already been observed in metals such as osmium,[20] graphene,[1] graphite,[21] and CNTs.[22] Graphite intercalation compounds (GICs) provide an ideal opportunity to examine phonons within the heavily electron-doped graphene sheets in these compounds, where the increased electronic density of states at the Fermi surface should make these effects more significant.

Recent theoretical work has shown that for most GICs the completely nonadiabatic zone-center phonon frequencies ω^{NA} are closer to the experimental values than the adiabatic frequencies ω^{A}. Using ω^{A} and ω^{NA} along with the experimental phonon frequency ω_{BWF}, Saitta *et al.*[18] calculate the contribution of the electron-phonon scattering to the phonon full width at half maximum γ_{σ}^{EPC}, which can be compared to the experimental width Γ. This formalism works quite well for KC_8 and CaC_6 but the width is overestimated in RbC_8. Furthermore LiC_6 and KC_{24} fall outside the boundaries of ω^{A} and ω^{NA}. We present a systematic experimental study of these effects within a particular family of GICs BaC_6, SrC_6, YbC_6, and CaC_6. The solid experimental trends presented here, and the interpretation thereof, can be applied widely within graphitic materials as the phonons we are measuring are the direct relative of the G mode in graphite, graphene, and CNTs. We choose samples with the same in-plane superlattice: BaC_6, SrC_6, YbC_6, and CaC_6. Changing the intercalant within these GICs controls the separation of the graphene sheets d, which provides a clear physical parameter linked to the changes in T_c in these compounds. Table I shows that as d decreases the superconducting transition temperature T_c increases dramatically. We show that reducing d, by changing the intercalant, leads to a softening of the C_z phonons modes, which is attributed to charge transfer into the π^* states. Using this, we go on to demonstrate that the C_{xy} phonon modes are strongly nonadiabatic, and that the size of these effects increases with increasing charge transfer to the π^* states. Furthermore, our work provides evidence that the size of the electron-phonon interaction is stronger than the current theory predicts.[18]

TABLE I. The values of d and the T_c for the GICs under consideration (Refs. 6, 7, 14, and 23).

	d (Å)	T_c (K)
BaC_6	5.25	$<$0.08
SrC_6	4.95	1.65
YbC_6	4.57	6.5
CaC_6	4.52	11.5

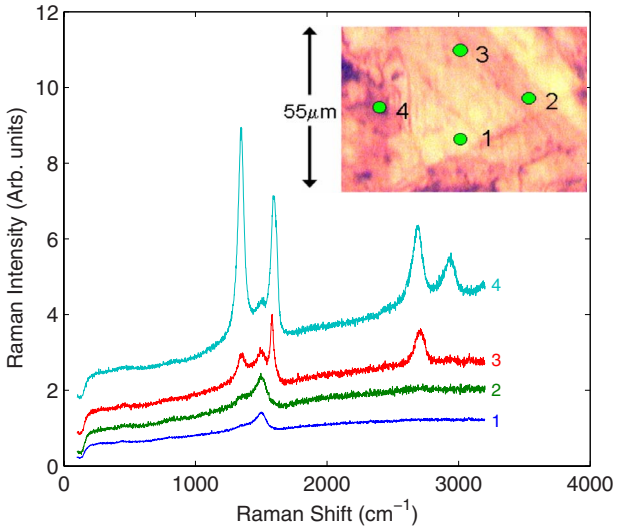

FIG. 1. (Color online) The Raman spectra from different positions numbered on the GIC surface shown in the increased-contrast inset. Spot 1 corresponds to pure, ordered GIC with one C_{xy} mode visible at ≈1500 cm^{-1}. Spots 2–4 also show the ≈1350 cm^{-1} and the ≈1600 cm^{-1} phonons which arise from sample disorder. All spectra are normalized to represent the same counting time.

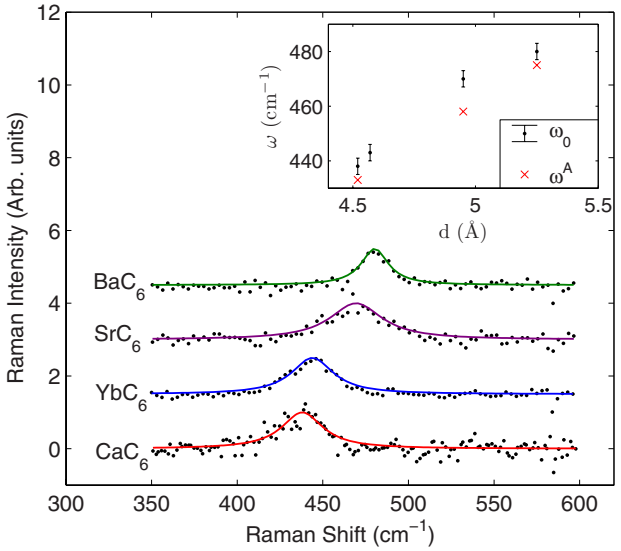

FIG. 2. (Color online) The Raman spectra of the C_z modes for BaC_6, SrC_6, YbC_6, and CaC_6. Black dots represent the data points and the solid lines are the Lorentzian fits. A smooth background has been removed from the data. The inset shows the variation in peak position for the experimental frequency ω_0 (dots) and the DFT value ω^A (crosses) (Ref. 13).

II. EXPERIMENTAL METHODS

Samples were synthesized using the vapor transport method[6,14] from natural Madagascan graphite flake. X-ray diffraction confirmed the phase purity of the samples, which were typically ~200 μm in size. For comparison CaC_6 and BaC_6 were also synthesized from highly oriented pyrolytic graphite (HOPG) using the Li alloy method.[24] The spectra were measured at room temperature using a Renishaw InVia confocal micro-Raman system, equipped with a 514.5 nm argon-ion laser, which was focused to ~3 μm onto the *ab* plane of the sample. The laser power at the sample was kept below 4 mW to avoid laser heating effects.

When dopant atoms are introduced into graphite, the in-plane C_{xy} mode of E_{2g} symmetry (also called the G mode), originally at ~1580 cm^{-1} in graphite and CNTs, softens and increases in linewidth. The new superlattice also folds a mode present at the *K* point in the graphite Brillouin zone to the Γ point, making it Raman active. This C_z mode, around 500 cm^{-1}, involves out-of-plane C motion.

Alkali and alkali-earth GICs react readily with oxygen and water.[25,26] The samples were therefore cleaved in an argon glove box (H_2O and O_2 levels <0.1 ppm) before being immediately transferred to prebaked quartz tubes and sealed under a vacuum of $<10^{-6}$ mbar.

The inset of Fig. 1 shows a typical increased-contrast image of the surface of the GICs considered here. While to the naked eye all samples look extremely shiny, under high magnification one can see and avoid step edges or small areas of surface degradation, which cause the surface to appear slightly blackened. This inhomogeneity explains why Refs. 27 and 28 observe contaminant peaks in most of their CaC_6 spectra. Only by choosing the most reflecting and therefore the most pure part of the sample (position 1 in Fig. 1) is a clean spectrum obtained containing a C_{xy} mode at ≈1500 cm^{-1} and a C_z mode at ≈450 cm^{-1} (too weak to see in this plot). We assign, in agreement with Ref. 27 the peaks at ≈1350 and ≈1600 cm^{-1} to disordered graphite to which small areas of the surface degrade. These contaminant peaks are inherently much more intense than the true GIC Raman peak because Raman scattering from disordered graphite is always a resonant process.[29,30] Reference 28 attributes the peak at ≈1350 cm^{-1} to disordered CaC_6. We note that this mode is not associated with the pristine surface.

III. RESULTS

The C_z modes from BaC_6, SrC_6, YbC_6, and CaC_6 are shown in Fig. 2. A clear trend in the peak positions is observed, with the peak softening from 480(3) cm^{-1} in BaC_6, 470(3) cm^{-1} in SrC_6, 443(3) cm^{-1} in YbC_6 to 438(3) cm^{-1} in CaC_6. To date, experimental phonon measurements of this family of GICs has been limited to CaC_6. Out-of-plane phonon dispersions below 50 meV have been measured by inelastic x-ray scattering,[31] and found to be close to the DFT predictions. Higher-energy modes above 50 meV have only been measured via Raman scattering, for CaC_6 Hlinka *et al.*[27] report ≈450 cm^{-1} and Mialitsin *et al.*[28] obtain 440 cm^{-1}.

The C_{xy} modes in GICs often possess the asymmetric Breit-Wigner-Fano (BWF) line shape,[25,26,32,33] which is modeled as a Raman signal intensity of

$$I(\omega) = I_0 \frac{\left(1 + \frac{\omega - \omega_{\mathrm{BWF}}}{q\Gamma/2}\right)^2}{1 + \left(\frac{\omega - \omega_{\mathrm{BWF}}}{\Gamma/2}\right)^2}, \quad (1)$$

where $1/q$ quantifies the asymmetry of the shape and ω_{BWF} and Γ are fitting parameters to the central frequency and full

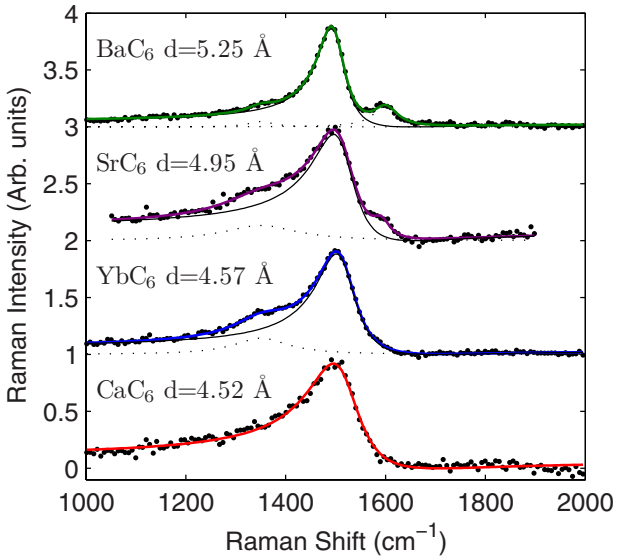

FIG. 3. (Color online) The Raman spectra of the C_{xy} modes for CaC_6, YbC_6, SrC_6, and BaC_6. Black dots are the measured spectrum, the thin line is the BWF function, the dotted lines are the surface contaminant and the fit is shown as a solid line. A linear background has been removed from the data and the spectra have been offset from one another for clarity.

width at half maximum, respectively. In the limit $1/q \to 0$ a Lorentzian line shape is recovered with a full width Γ and frequency ω_0. Typical Raman spectra of the C_{xy} modes for the samples considered here are shown in Fig. 3. The BWF line shape [Eq. (1)] was used to fit the peak and Lorentzian functions were also included in some fits to account for any small contamination from the D and G modes. The errors were estimated by fitting a number of different spectra. Table II provides a list of the fitting parameters. The data for CaC_6 are in excellent agreement with Hlinka *et al.*[27] who report $\omega_{\mathrm{BWF}}=1511\ \mathrm{cm}^{-1}$, $\Gamma=111\ \mathrm{cm}^{-1}$, and $1/q=0.28$. Mialitsin *et al.*[28] measure a spectrum at 20 K showing large D and G peaks. They describe a Lorentzian line shape with $\omega_0=1508\ \mathrm{cm}^{-1}$ and $\Gamma=76\ \mathrm{cm}^{-1}$.

IV. ANALYSIS AND DISCUSSION OF RESULTS

The trend in the C_z modes to soften from BaC_6, SrC_6, YbC_6, to CaC_6 clearly depends on d rather than the intercalant mass. We propose that by increasing d charge is transferred out of the π^* band depopulating the Dirac cones. As the π^* band is antibonding filling it with electrons destabilizes the bonds causing the softening of the phonons, thus these modes are sensitive to charge transfer. Boeri *et al.*[34] predict C_z modes soften considerably when charge is transferred into the π^* states in jellium intercalated graphite. The inset of Fig. 2 compares the peak values to adiabatic DFT calculations.[13] Theory predicts that the difference between ω^A and ω^{NA} is due to intraband electron-phonon scattering, as interband process contribute equally to ω^A and ω^{NA}.[3] Given that the experimental values are close to ω^A, and assuming that the $|\boldsymbol{q}.\boldsymbol{v}_F| \ll \omega$ condition is fulfilled, this agreement shows that there is very little renormalization of these modes due to intraband transitions. In addition the linewidths of these modes are relatively small and, within the experimental errors, show no trends with d. The strong doping sensitivity of the C_z modes means that the experimental frequency can be used, in conjunction with DFT, to infer a bulk value of the charge transfer. The experimental value for CaC_6 of $438(3)\ \mathrm{cm}^{-1}$ is close to the DFT prediction of $433\ \mathrm{cm}^{-1}$.[13] In this model 0.20 electron per C atom[35] are found in the π^* states, which is close to the angle-resolved photoemission spectroscopy (ARPES) derived value of 0.22.[16] This supports the view that the charge transfer in the surface layers probed in ARPES is representative of the bulk, and shows that these techniques are consistent in this regard. The charge-transfer dependence proposed here also explains the series of GICs CsC_8, RbC_8 to KC_8,[36] which show a similar trend. The gradient of these effects is similar, but the overall values are different, since in XC_8 GICs (where X =intercalant) the charge transfer is less. We also note that in XC_8 GICs the C_z mode is folded from M in the graphite Brillouin zone, whereas for IC_6 GICs the mode is folded from K, which is at slightly lower energy.

The ω_{BWF} values shown in Table II show no dependence on intercalant mass: these phonons only sample the environment of the (doped) graphene planes. These values are all significantly different to the values predicted using DFT (Ref. 18) with the adiabatic approximation ω^A (see Table II). In fact, the values are closer to the completely nonadiabatic limit ω^{NA}, which demonstrates that nonadiabatic effects are essential to understand these phonon energies. The degree of nonadiabaticity, may be estimated by $\omega_{\mathrm{BWF}}-\omega^A$ which increases as charge is transferred to the π^* states in BaC_6, SrC_6 to CaC_6. Despite the similarity in ω_{BWF}, Γ varies significantly increasing in the order BaC_6, $SrC_6 \approx YbC_6$ to CaC_6. This is indicative of a decrease in phonon lifetime as charge is transferred into the π^* states. The trends observed when doping the π^* states by changing the intercalant atom in GICs are different to those measured in graphene and metallic CNTs at the much lower doping levels accessed by elec-

TABLE II. The fit parameters for the C_{xy} mode of the GICs considered here. Values in columns ω^A and ω^{NA} correspond to the DFT calculations of Ref. 18. All values except $1/q$ are in cm^{-1}.

	ω_{BWF}	Γ	$1/q$	ω^A	ω^{NA}	σ	γ_σ^{EPC}
BaC_6	1510(5)	70(10)	−0.25(5)	1462	1521	700(200)	46(8)
SrC_6	1510(5)	100(10)	−0.30(5)	1459	1530	910(160)	64(5)
YbC_6	1515(5)	100(10)	−0.30(5)				
CaC_6	1510(3)	120(10)	−0.35(5)	1446	1529	790(80)	70(4)

trostatic gating.[1] These systems show an increase in phonon energy and a decrease in Γ with electron doping. However, different effects are present in the high doping case of the GICs because the Kohn anomaly which exists near $\boldsymbol{q}=0$ in graphene[3] is displaced to finite $\boldsymbol{q}$ and the π^* band is altered and is accompanied by other intercalant-related bands.[11,13,25,34]

Within Saitta *et al.*'s theory ω_{BWF} should fall in between the completely adiabatic limit ω^A and the completely nonadiabatic limit ω^{NA}. The electron-scattering rate $\sigma=\hbar/\tau$, where τ is the electron momentum-relaxation time controls where ω_{BWF} falls in between these limits. For $\sigma \gg \omega^A$ we find $\omega_{\mathrm{BWF}} \rightarrow \omega^A$ and for $\sigma \ll \omega^A$ the system becomes fully nonadiabatic and $\omega_{\mathrm{BWF}} \rightarrow \omega^{NA}$. We observe no systematic trend in σ, and we find the values are highly sensitive to any small errors in the experimental and theoretical frequencies. It is therefore difficult to use this method to accurately extract the electron-scattering rate. It is however, possible to rearrange Saitta *et al.*'s equations for derive the electron-phonon-scattering induced linewidth

$$\frac{\gamma_\sigma^{EPC}}{2} \simeq \sqrt{(\omega_{\mathrm{BWF}}-\omega^A)(\omega^{NA}-\omega_{\mathrm{BWF}})}. \quad (2)$$

The derived values of γ_σ^{EPC} account for the trend in Γ to increase going from BaC_6, SrC_6 to CaC_6, but significantly underestimate its absolute value. The Γ values reported here should be the intrinsic linewidth in these GICs, with a negligible disorder contribution, as these results are reproducible in samples produced from Madagascan flake graphite and HOPG. This is despite HOPG having a crystallite size of ~ 1 μm, far smaller than the ~ 100 μm in Madagascan flake graphite. An order of magnitude calculation can be performed to estimate the length scales which correspond to the observed Γ. The C_{xy} modes in these GICs have a typical lifetime of $\omega_{\mathrm{BWF}}/\Gamma \approx 15$ periods and stretch bonds over ~ 5 Å, which implies the atomic motion is correlated over only ~ 80 Å. Madagascan flake based CaC_6 and YbC_6 samples made in the same way as the samples used in this study have ordered regions of ~ 50 μm.[37] Furthermore, the mean distance between scattering centers, as estimated from the low-temperature resistivity is ~ 1000 Å.[10] Disorder broadening should therefore have an insignificant role here. Anharmonic effects are also unlikely to cause such a large linewidth.[18] We therefore suggest that theory underestimates the degree of electron-phonon interaction in these compounds.[18]

These results also have implications for the debate outlined in Sec. I regarding which phonons and electrons are most relevant for the superconductivity in SrC_6, YbC_6 and CaC_6. The trend uncovered that T_c increases when charge is transferred into the graphene layers provides strong evidence that the C phonons and the π^* electrons are involved in the superconductivity. This is very difficult to reconcile with the isotope effect measurements[8] and early theory,[12] which suggest that superconductivity is predominately due to the intercalant atoms. Our work supports the assertion that the C atoms are relevant, either the C_z modes[11,13,14] or the C_{xy} modes.[16]

V. CONCLUSIONS

In conclusion, we present phonon measurements of BaC_6, SrC_6, YbC_6, and CaC_6. Raman spectroscopy is employed to monitor the systematic changes in both the phonons and the electron-phonon interaction in the graphene sheets as d is varied by changing the intercalant atom. The C_z phonons are found to soften in the order BaC_6, SrC_6, YbC_6 to CaC_6 indicative of change transfer into the π^* states as d is reduced. Concurrent with this charge transfer is a large increase in T_c. While the out-of-plane carbon mode is well described within the Born-Oppenheimer approximation, the in-plane carbon mode is not. We demonstrate that the in-plane carbon modes show strong nonadiabatic effects, which lead to phonon frequencies that are considerably higher than the adiabatic prediction. As the charge transfer to the π^* states increases, these effects get stronger causing an increasing discrepancy between the adiabatic prediction and experimental frequency and an increase in the phonon linewidth. Theoretical work (Ref. 18) anticipates the relevance of the nonadiabatic effects in these GICs. However, our work provides evidence that the degree of electron-phonon interaction for this mode is stronger than the current theory predicts. Nonadiabatic effects can be used to extract information on the electrons, phonons, and the electron-phonon interaction within the doped graphene layers, which constitute these compounds. Through a systematic study of XC_6 GICs, we identify trends which should be widely applicable to characterize a range of graphitic compounds using Raman spectroscopy.

ACKNOWLEDGMENTS

We thank the EPSRC, COST ECOM P16, Selwyn College and Jesus College for funding and the University College London Chemistry Department, G. Srinivas, S. Firth, and S. Albert-Seifried for experimental assistance. We also thank M. Calandra, A. M. Saitta, F. Mauri, F. Fernandez-Alonso, P. B. Littlewood, A. C. Walters, M. Sutherland, and S. Bhattacharya for discussions.

*mpmd2@cam.ac.uk

[1] S. Pisana, M. Lazzeri, C. Casiraghi, K. S. Novoselov, A. K. Geim, A. C. Ferrari, and F. Mauri, Nature Mater. **6**, 198 (2007).
[2] A. Das, S. Pisana, B. Chakraborty, S. Piscanec, S. K. Saha1, U. V. Waghmare, K. S. Novoselov, H. R. Krishnamurthy, A. K. Geim, A. C. Ferrari, and A. K. Sood, Nat. Nanotechnol. **3**, 210 (2008).
[3] M. Lazzeri and F. Mauri, Phys. Rev. Lett. **97**, 266407 (2006).
[4] J. C. Tsang, M. Freitag, V. Perebeinos, J. Liu, and P. Avouris, Nat. Nanotechnol. **2**, 725 (2007).
[5] M. Lazzeri, S. Piscanec, F. Mauri, A. C. Ferrari, and J. Robertson, Phys. Rev. B **73**, 155426 (2006).

[6] T. E. Weller, M. Ellerby, S. S. Saxena, R. P. Smith, and N. T. Skipper, Nat. Phys. **1**, 39 (2005).
[7] N. Emery, C. Hérold, M. d'Astuto, V. Garcia, C. Bellin, J. F. Marêché, P. Lagrange, and G. Loupias, Phys. Rev. Lett. **95**, 087003 (2005).
[8] D. G. Hinks, D. Rosenmann, H. Claus, M. S. Bailey, and J. D. Jorgensen, Phys. Rev. B **75**, 014509 (2007).
[9] G. Lamura, M. Aurino, G. Cifariello, E. Di Gennaro, A. Andreone, N. Emery, C. Hérold, J. Marêché, and P. Lagrange, Phys. Rev. Lett. **96**, 107008 (2006).
[10] M. Sutherland, N. Doiron-Leyraud, L. Taillefer, T. Weller, M. Ellerby, and S. S. Saxena, Phys. Rev. Lett. **98**, 067003 (2007).
[11] M. Calandra and F. Mauri, Phys. Rev. Lett. **95**, 237002 (2005).
[12] I. I. Mazin, Phys. Rev. Lett. **95**, 227001 (2005).
[13] M. Calandra and F. Mauri, Phys. Rev. B **74**, 094507 (2006).
[14] J. S. Kim, L. Boeri, J. R. O'Brien, F. S. Razavi, and R. K. Kremer, Phys. Rev. Lett. **99**, 027001 (2007).
[15] K. Sugawara, T. Sato, and T. Takahashi, Nat. Phys. **5**, 40 (2009).
[16] T. Valla, J. Camacho, Z.-H. Pan, A. V. Fedorov, A. C. Walters, C. A. Howard, and M. Ellerby, Phys. Rev. Lett. **102**, 107007 (2009).
[17] S. Baroni, S. de Gironcoli, A. Dal Corso, and P. Giannozzi, Rev. Mod. Phys. **73**, 515 (2001).
[18] A. M. Saitta, M. Lazzeri, M. Calandra, and F. Mauri, Phys. Rev. Lett. **100**, 226401 (2008).
[19] S. Engelsberg and J. R. Schrieffer, Phys. Rev. **131**, 993 (1963).
[20] Yu. S. Ponosov, G. A. Bolotin, C. Thomsen, and M. Cardona, Phys. Status Solidi B **208**, 257 (1998).
[21] K. Ishioka, M. Hase, M. Kitajima, L. Wirtz, A. Rubio, and H. Petek, Phys. Rev. B **77**, 121402(R) (2008).
[22] A. W. Bushmaker, V. V. Deshpande, S. Hsieh, M. Bockrath, and S. B. Cronin, Nano Lett. **9**, 607 (2009).
[23] S. Nakamae, A. Gauzzi, F. Ladieu, D. L'Hote, N. Emery, C. Hérold, J. Marêché, P. Lagrange, and G. Loupias, Solid State Commun. **145**, 493 (2008).
[24] S. Pruvost, C. Hérold, A. Hérold, and P. Lagrangea, Carbon **42**, 1825 (2004).
[25] M. S. Dresselhaus and G. Dresselhaus, Adv. Phys. **51**, 1 (2002).
[26] T. Enoki and M. Endo, *Graphite Intercalation Compounds and Applications* (Oxford University Press, New York, 2003).
[27] J. Hlinka, I. Gregora, J. Pokorny, C. Hérold, N. Emery, J. F. Marêché, and P. Lagrange, Phys. Rev. B **76**, 144512 (2007).
[28] A. Mialitsin, J. S. Kim, R. K. Kremer, and G. Blumberg, Phys. Rev. B **79**, 064503 (2009).
[29] M. A. Pimenta, G. Dresselhaus, M. S. Dresselhaus, L. G. Cançado, A. Jorio, and R. Saito, Phys. Chem. Chem. Phys. **9**, 1276 (2007).
[30] A. C. Ferrari, Solid State Commun. **143**, 47 (2007).
[31] M. H. Upton, A. C. Walters, C. A. Howard, K. C. Rahnejat, M. Ellerby, J. P. Hill, D. F. McMorrow, A. Alatas, B. M. Leu, and W. Ku, Phys. Rev. B **76**, 220501(R) (2007).
[32] R. J. Nemanich, S. A. Solin, and D. Gúerard, Phys. Rev. B **16**, 2965 (1977).
[33] P. C. Eklund and K. R. Subbaswamy, Phys. Rev. B **20**, 5157 (1979).
[34] L. Boeri, G. B. Bachelet, M. Giantomassi, and O. K. Andersen, Phys. Rev. B **76**, 064510 (2007).
[35] M. Calandra (private communication).
[36] P. C. Eklund, G. Dresselhaus, M. S. Dresselhaus, and J. E. Fischer, Phys. Rev. B **16**, 3330 (1977).
[37] A. C. Walters (private communication).